



Molecular Crystals and Liquid Crystals Science and Technology. Section A. Molecular Crystals and Liquid Crystals

Publication details, including instructions for authors and
subscription information:

<http://www.tandfonline.com/loi/gmcl19>

Bend Orientational Diffusivity Measurement by Light Beating Spectroscopy in a Disk-like Thermotropic Nematic Phase (N_D)

T. Othman ^a, M. M. Jebari ^a, A. Gharbi ^a & G. Durand ^b

^a Laboratoire de Physique des Cristaux Liquides et des
Polymères, Faculté des Sciences de, Tunis-Campus Universitaire
Le, Belvedere, 1060, Tunisie

^b Laboratoire de Physique des Solides, Université de Paris-Sud,
Bat. 510, 91405, Orsay, Cedex, France

Version of record first published: 04 Oct 2006.

To cite this article: T. Othman , M. M. Jebari , A. Gharbi & G. Durand (1996): Bend Orientational
Diffusivity Measurement by Light Beating Spectroscopy in a Disk-like Thermotropic Nematic Phase
(N_D), Molecular Crystals and Liquid Crystals Science and Technology. Section A. Molecular Crystals
and Liquid Crystals, 281:1, 145-153

To link to this article: <http://dx.doi.org/10.1080/10587259608042240>

PLEASE SCROLL DOWN FOR ARTICLE

Full terms and conditions of use: <http://www.tandfonline.com/page/terms-and-conditions>

This article may be used for research, teaching, and private study purposes. Any
substantial or systematic reproduction, redistribution, reselling, loan, sub-licensing,
systematic supply, or distribution in any form to anyone is expressly forbidden.

The publisher does not give any warranty express or implied or make any
representation that the contents will be complete or accurate or up to date. The
accuracy of any instructions, formulae, and drug doses should be independently
verified with primary sources. The publisher shall not be liable for any loss, actions,

claims, proceedings, demand, or costs or damages whatsoever or howsoever caused arising directly or indirectly in connection with or arising out of the use of this material.

Bend Orientational Diffusivity Measurement by Light Beating Spectroscopy in a Disk-like Thermotropic Nematic Phase (N_D)

T. OTHMAN, M. M. JEBARI and A. GHARBI

Laboratoire de Physique des Cristaux Liquides et des Polymeres, Faculté des Sciences de Tunis-Campus Universitaire Le Belvedere 1060 Tunisie

G. DURAND

Laboratoire de Physique des Solides, Université de Paris-Sud, Bat. 510, 91405 Orsay, Cedex, France

(Received July 10, 1995; in final form October 11, 1995)

Using a light-beating technique for an appropriate scattering geometry, we have measured the bend orientational diffusivity (D_{bend}) for an "hexa-n-alcanoyloxytruxene" ($\text{HATXC}_{12}\text{H}_{23}$) sample which exhibits a disk-like thermotropic nematic phase (N_D) between 57°C and 84°C. From K_{33} measurement by the Frederiks method, the bend viscosity (η_{bend}) is deduced. It is about 100 times higher than those corresponding to rod-like thermotropic nematics. From previous measurements of D_{splay} and D_{twist} for $\text{HATXC}_{12}\text{H}_{23}$, we have deduced the elastic constants (K_{11} , K_{22}) and the viscosities (η_{splay} , η_{twist}). It has been concluded that, although there is a difference between the two kinds of molecules (disk-like and rod-like), the backflow has the same effect as in rod-like nematic phase.

Keywords: *Disk-like, thermotropic, diffusivity.*

On the one hand, it is well known that for a rod-like nematic (N_B) phase, orientational diffusivity coefficients, D_{splay} and D_{twist} , corresponding, respectively, to splay and twist deformations, are of the same order of magnitude. However, the coefficient D_{bend} , corresponding to bend distortion, exhibits a large deviation with respect to the two previous coefficients D_{twist} and D_{splay} .¹ This behavior is generally attributed to the backflow effects. The latter are known to reduce the bend viscosity compared with the twist one. On the other hand, in a discotic nematic phase (N_D), the constituent molecules have flat or nearly flat cores surrounded by relative long chains.² The director which denotes the preferred average orientation is closely parallel to disk-normals (or molecular short axis). In contrast to this behavior, the director, for rod-like molecule, lies along the molecule long axis. Therefore, based on the different structures of N_D and N_B , one expects an exchange between splay and bend deformations. Consequently, a large deviation between D_{splay} and D_{twist} is expected (the symmetry axis is along the larger dimension of the molecule for N_B , while it is along the shorter one for N_D). In a previous work,³ the authors have investigated a disk-like nematic

(N_D) lyotropic phase and have measured the orientational diffusivities D_{splay} and D_{twist} . They found a divergence between these two constants. They attributed this divergence to the backflow effects which reduce the splay viscosity compared with the twist one. To support the idea of exchange between splay and bend distortion, a D_{bend} measurement is essential. Due to experimental limitations, they did not measure the bend orientational diffusivity (D_{bend}), and simply anticipated that the backflow reduction must be very weak in the case of bend distortion, based on geometrical considerations.

In a previous report,⁴ we presented measurements of D_{splay} and D_{twist} for a discotic thermotropic nematic liquid crystal (LC). Contrary to what had been reported for discotic lyotropic nematic phases, D_{splay} and D_{twist} are in same order of magnitude and exhibit the same ratio as in rod-like nematic phase for which $D_{\text{splay}}/D_{\text{twist}}$ ratio is of order of 1. Therefore a distinction between bend and twist viscosities must be expected. In order to provide a quantitative comparison between discotic and rod-like nematic phase about orientational diffusivities, we performed a measurement of orientational diffusivity D_{bend} on a discotic thermotropic nematic phase. In addition, measurements of the curvature Frank elastic constant (K_{33}) using the Frederiks transition is also performed. Consequently, we show that in a combination of our measurements and a theoretical calculation of elastic constant ratios,⁵ the numerical values of the three constants (K_{11} , K_{22} , K_{33}) and the viscosities (η_{splay} , η_{twist} , η_{bend}) can be deduced.

We start with a short introduction of the theoretical concepts used in the present study. Then we describe the experimental procedure: technique, materials. In the last section, we present the data along with a discussion and a comparison with the nematic N_B .

It has long been known that in a nematic liquid crystal, the long range orientational order is subject to thermal fluctuations about the equilibrium direction.^{6,7,8} To get information on the dynamical behavior of these fluctuations, we use the light beating technique to measure the relaxation time of these thermal fluctuations. We choose a coordinate system (\mathbf{o} , \mathbf{x} , \mathbf{y} , \mathbf{z}) in which the mean direction \mathbf{n}_0 lies along \mathbf{z} axis, \mathbf{e}_1 and \mathbf{e}_2 are two unit vectors lying, respectively, along \mathbf{x} and \mathbf{y} axis (Fig. 1). The wave vector $\mathbf{q} = \mathbf{K}_i - \mathbf{K}_s$ is in the (\mathbf{x} , \mathbf{z}) plane, with \mathbf{K}_i and \mathbf{K}_s being, respectively, the incident and scattered wave vectors. The local director \mathbf{n} position is dependent in the sample; it may be expressed as:

$$\mathbf{n}(\mathbf{r}) = \mathbf{n}_0 + \delta n_1 \mathbf{e}_1 + \delta n_2 \mathbf{e}_2$$

The mode δn_1 is a combination of bend and splay deformations, while the mode δn_2 is a combination of bend and twist deformations.

For either mode, at a fixed \mathbf{q} , the relaxation rate Γ_i is proportional to q^2 and can be expressed as:

$$\Gamma_i = \frac{1}{\eta_i(\mathbf{q})} [K_{ii} q_{\perp}^2 + K_{33} q_{\parallel}^2] \quad (1)$$

where i denotes the mode of fluctuation δn parallel ($i = 1$) or normal ($i = 2$) to the (\mathbf{q} , \mathbf{n}_0) plane. K_{11} , K_{22} and K_{33} are the Frank elastic constants characterizing splay, twist and

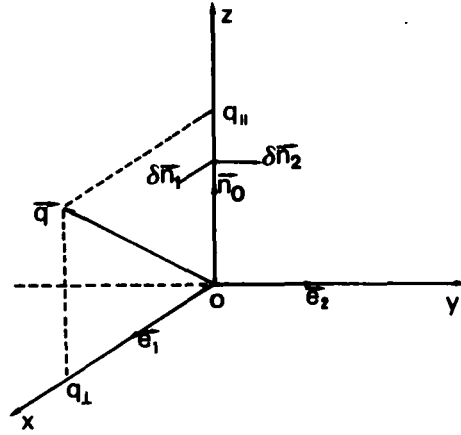


FIGURE 1 Fluctuation modes: The δn_1 mode which is in the $(\mathbf{q}, \mathbf{n}_0)$ plane is a combination of the bend and splay deformation. The δn_2 mode which is perpendicular to the $(\mathbf{q}, \mathbf{n}_0)$ plane is a combination of bend and twist deformation. \mathbf{n}_0 is the equilibrium direction.

bend deformations respectively; $\eta_1(\mathbf{q})$ and $\eta_2(\mathbf{q})$ are the viscosities associated with the modes 1 and 2; q_\perp and q_\parallel denote the perpendicular and parallel components of the wave vector \mathbf{q} with respect to \mathbf{n}_0 .

In order to describe how to measure the pure bend orientational diffusivity ($D_{\text{bend}} = K_{33}/\eta_{\text{bend}}$), we consider a homeotropic sample confined between two glass plates separated by a distance d (a monodomain of thickness d). Then, we choose the appropriate scattering geometry in which \mathbf{q} must be along the z axis (or director \mathbf{n}_0), Figure 2. In this situation, the scattered light when it exists, must be centered outside the sample on the transmitted (or reflected) illuminating beam because reflection and refraction across the plates, limiting the sample, conserve the tangential component of light wave vectors along this interface.

Because the sample has a finite size, the distortion modes of wave vector q_z along \mathbf{n}_0 (or z axis) are quantized, with $q_z(p) = p\pi/d$, where p is an integer, and d is the sample thickness.⁹ Consequently, a large Rayleigh scattering is expected only when $q_1^{\text{opt}} = q_z$, where $q_1^{\text{opt}} = \mathbf{K}_i - \mathbf{K}_s$ is an optical wave vector which must be distinguished from mechanical wave vector q_z . From light propagation laws and for an ordinary incident light and extraordinary scattered one, we can calculate q_1^{opt} from the following expressions:

$$q_1^{\text{opt}} = (n_0 \cos \alpha - n \cos \beta) 2\pi/\lambda \quad (2)$$

$$n_0 \sin \alpha = n \sin \beta \quad (3)$$

where α, β are respectively the incidence and scattering angles in the sample (see Fig. 2). The extraordinary index n at an angle β , is given by the usual relationship, $n^{-2} = (\cos^2 \beta) n_0^{-2} + (\sin^2 \beta) n_e^{-2}$. λ is the incident light wavelength.

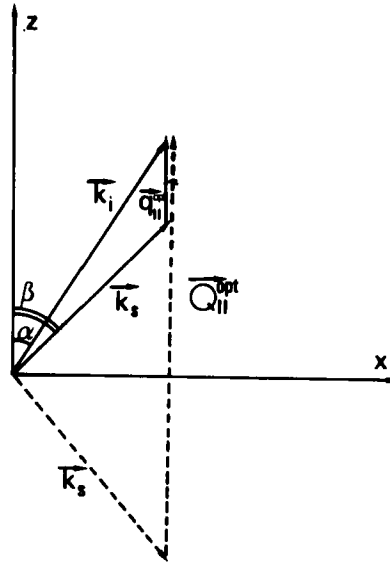


FIGURE 2 Scattering geometry: $q_{\parallel}^{\text{opt}}$ and $Q_{\parallel}^{\text{opt}}$ correspond respectively to forward and backward scattering. \mathbf{k}_i and \mathbf{k}_s are the incoming and the scattering wave vectors. z denotes the preferred average orientation.

This system has two solutions:

$$q_{\parallel}^{\text{opt}} = [n_0 \cos \alpha - n_0^2 n_e^{-2} \sin^2 \alpha]^{1/2} 2\pi/\lambda$$

for the forward scattering, along the transmitted beam, and

$$Q_{\parallel}^{\text{opt}} = [n_0 \cos \alpha + n_0^2 n_e^{-2} \sin^2 \alpha]^{1/2} 2\pi/\lambda$$

for the backward scattering, along the reflected beam (Fig. 2). In the case where $q_{\parallel}^{\text{opt}}$ (or $Q_{\parallel}^{\text{opt}}$) coincides exactly with $q_z(p)$, we define a discrete set of incidence angles α_p for which there is a large scattered light.

In the general case (see Ref. 9) and for an homeotropic liquid crystal, the differential scattering cross section is given by:

$$\begin{aligned} \frac{d^2 \sigma}{d\omega d\Omega} &\propto \int_{-d/2}^{+d/2} \sum_{m, q_z} \langle |\delta n_m(q_z)|^2 \rangle \exp [i(q_{\parallel}^{\text{opt}} - q_z)z] dz \\ &= d \sum_{m, q_z} \langle |\delta n_m(q_z)|^2 \rangle \frac{\sin(q_{\parallel}^{\text{opt}} - q_z) \frac{d}{2}}{(q_{\parallel}^{\text{opt}} - q_z) \frac{d}{2}} \end{aligned} \quad (4)$$

where q_z is $q_z(p)$ and m takes on the value 1 and 2 for the modes described above.

We see that the finite sample size leads to an uncertainty in the selection of $q_z(p)$ (single slit interference function in Eq. (4)). This means that more than one mode $q_z(p)$ contributes to the scattered light in a given direction β . The predominant modes are those within the interval:

$$q_{\parallel}^{\text{opt}} - 2\pi/d < q_z(p) < q_{\parallel}^{\text{opt}} + 2\pi/d \quad (5)$$

This yields a smoothing of the angular distribution of the scattered light which is sufficient to explain why, in practice, we did not observe the fringes despite the expected discrete spectrum. So, we can study the Rayleigh scattered light corresponding to bend deformation without the necessity for an exact coincidence of $q_{\parallel}^{\text{opt}}$ (or $Q_{\parallel}^{\text{opt}}$) and $q_z(p)$. We remark that when d increases, the angular spacing between the modes becomes small. Consequently, the difference between q^{opt} and $q_z(p)$ decreases. Also, the uncertainty in the selection of q_z decreases.

The material used here is the “hexa-*n*-alcanoyloxytruxene” (HATXC₁₂H₂₅) which exhibits a disk-like thermotropic nematic phase (N_D) between 57°C and 84°C.¹⁰ The thickness of the sample is given by the mica spacer to 120 μm . We select a temperature of 65°C. To obtain a good homeotropic orientation (\mathbf{n}_0 perpendicular to the plates), we use the same method as in Ref. 4. The sample is placed on a goniometer which allows us to vary the incidence air angle α_a (angle between \mathbf{n}_0 and \mathbf{K}_i) from 19°C to 47°C. The incident light at $\lambda = 632.8 \text{ nm}$ is provided by a 10 MW He-Ne laser. Its polarization is chosen ordinary (or vertically) by a linear polarizer placed in front of the sample. A cooled S₂₀ photomultiplier (PM) is fixed on a rotatable arm which can be rotated in a plane orthogonal to the vertical goniometer axis. It allows us to collect the light along the scattered direction \mathbf{K}_s at an air angle $\beta_a \approx \pi - \alpha_a$ (close to the reflected beam; see Fig. 2). The scattered light passes through a horizontal linear analyser. Note that in this situation the geometrical factor $(i_2 f_z + i_z f_2)^2$, which defines the selection rules¹ is equal to $\sin^2 \alpha_a$. A pinhole of radius 50 μm placed in front of the photomultiplier allows collection of the scattered light over less than one coherence area. The photocurrent $i(t)$ coming from the PM is sent to a 64 channel digital correlator, which is interfaced with a computer to collect and analyse the autocorrelation function $C_i(t)$. In the absence of multiple scattering, $C_i(t)$ has the following simple expression:¹¹

$$C_i(t) = (i_o + i_s)^2 + i_s^2 \exp(-2t/\tau) + 2i_o i_s \exp(-t/\tau)$$

where i_s is the intensity of the signal coming from the fluctuations of the nematic director \mathbf{n}_0 , i_o is the “local oscillator” intensity when using heterodyne detection and $\tau = 1/Dq^2$ is the damping time. In a purely heterodyne regime ($i_s \ll i_o$), the autocorrelation function $C_i(t)$ is reduced to a single exponential decay with a characteristic time $\tau_c = \tau$. If the regime is purely homodyne ($i_o \sim 0$), $C_i(t)$ is also reduced to a single exponential but with a characteristic time $\tau_c = \tau/2$. From a fit of the experimental autocorrelation function with two exponentials, $A \exp(-2t/\tau) + B \exp(-t/\tau) + C$, we obtain the damping time τ . The experimental constants A , B are deduced from a fit to the experimental $C_i(t)$, while C is kept fixed to the measured baseline. The orientational diffusivity, D_{bend} , is deduced from a plot of τ^{-1} vs. $q_z^2(p)$. Note that $q_z(p)$ is close to $Q_{\parallel}^{\text{opt}}$ corresponding to each angle α_a . The integer p varies from 1108 (for $\alpha_a = 19^\circ$) to 976

(for $\alpha_a = 47^\circ$). A straight line fits the experimental data as shown in Figure 3. From the slope we deduce the bend orientational diffusivity (D_{bend}): $D_{\text{bend}} = 1.26 \cdot 10^{-8} \text{ cm}^2/\text{s}$. It is about 2 order of magnitude smaller than the one for rod-like molecules. This difference may be attributed to higher bend viscosity (η_{bend}). To confirm this claim, we performed an independent measurement of the bend Frank elastic constant K_{33} using Frederiks transition. In this experiment, we used a homeotropic sample, confined between two parallel glass plates coated with conducting layers. The sample thickness which is equal to $60 \mu\text{m}$ was measured by an interferometric method. Then the sample is placed between two crossed polarizers which allow us to examine the macroscopic distortions of the common direction. In the presence of the applied electric field which is weaker than the threshold one, no transmitted light intensity is measured. This is in agreement with a good quality homeotropic preparation. Gradually increasing the applied voltage, a weak transmitted intensity is observed at a $v \approx 3.7$ volts. It reflects the presence of a weak distortion of the director \mathbf{n}_0 . From the threshold voltage $v \approx 3.7$ volts and the value of the anisotropy of the dielectric constant¹² $|\epsilon_a| \approx 0.2$, we deduce a value for K_{33} : $K_{33} \approx 0.22 \cdot 10^{-6}$ dynes. From this value and using the relation $D_{\text{bend}} = K_{33}/\eta_{\text{bend}}$, one can deduce the bend viscosity (η_{bend}): $\eta_{\text{bend}} \approx 18 \text{ p}$.

We would like to mention that for this homeotropic geometry, and using the electro-optic method, we can only measure the K_{33} elastic constant. To measure the other two elastic constants K_{11} and K_{22} corresponding respectively to splay and twist deformations, a planar or homeoplanar orientation of the sample is essential. This orientational geometry is easily obtained in the case of rod-like molecules (N_B). In this way, we have tried several orientation techniques in order to prepare a cell with either planar or homeoplanar oriented regions for disk-like molecules (application of a static magnetic field, coating the cell faces with an organic agent, using the shear method, which was used in columnar discotic case). Unfortunately, all these methods do not give

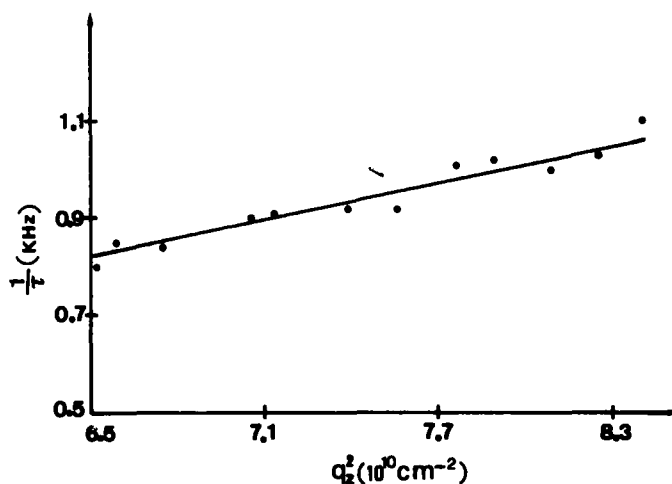


FIGURE 3 Relaxation rates $1/\tau$ versus q_z^2 : q_z is the mechanical wave vector given by $q_z(p) = p\pi/d$.

satisfactory results. Due to these orientational difficulties, we have not measured the elastic constants K_{11} and K_{22} .

In Table I, we report the orientational diffusivity coefficients (D_{splay} , D_{twist} and D_{bend}) measured at 65°C for the truxene ($\text{HATXC}_{12}\text{H}_{25}$). We remark that the ratio $D_{\text{splay}}/D_{\text{twist}}$ is close to 1, while $D_{\text{bend}}/D_{\text{twist}}$ is about 3. One can deduce that the backflow effect is more important in the bend distortion than in the splay one. For comparison, we report in the same table, these values measured previously for a discotic lyotropic nematic phase³ and for a conventional thermotropic nematic phase liquid crystal N-(*p*-methoxybenzylidene)-*p*-butylamine, MBBA.¹ The difference between D_{splay} and D_{twist} for a discotic lyotropic nematic has been attributed to the backflow effect. The latter reduce the splay viscosity compared with the twist one. However this would not be the case for the rod-like nematic phase, since the divergence occurs between D_{twist} and D_{bend} . About the orientational diffusivity coefficients, the truxene ($\text{HATXC}_{12}\text{H}_{25}$) presents the same behavior as for the rod-like nematic although there is a difference between the geometrical shape of the two kinds of molecules.

Because of the orientation difficulties mentioned above concerning the K_{11} and K_{22} measurements, one can use the measured value of K_{33} and the calculated ratios:⁵ $K_{22}/K_{33} \sim 5$; $K_{11}/K_{33} \sim 2$, to estimate $K_{11} \approx 0.45 \cdot 10^{-6}$ dynes and $K_{22} \approx 1.1 \cdot 10^{-6}$ dynes. Furthermore, the results of measurements¹³ of the ratio K_{11}/K_{33} for two truxene derivatives in nematic phases: hexa(decanoyloxy)truxene and hexa(tetradecanoyloxy)truxene, prove the validity of the theoretical predictions.⁵ So, the authors¹³ found $K_{11} > K_{33}$ in the whole temperature range. For this reason we have used the calculated ratios⁵ to estimate K_{11} and K_{22} , since our sample ($\text{HATXC}_{12}\text{H}_{25}$) is a truxene derivative. For comparison we report in Table II the K_{11} , K_{22} and K_{33} values corresponding to $\text{HATXC}_{12}\text{H}_{25}$ and those corresponding to MBBA. We remark that the elastic constants K_{11} , K_{22} and K_{33} are all in the same order of magnitude for $\text{HATXC}_{12}\text{H}_{25}$ and MBBA. The order $K_{22} < K_{11} < K_{33}$ which is always observed for rod-like molecules comes $K_{33} < K_{11} < K_{22}$ for disk-like molecules. The elastic constants interchange their role, since K_{33} is smaller for $\text{HATXC}_{12}\text{H}_{25}$. This result implies that it is more difficult to twist a plane of disk-like molecules with respect to a neighboring plane, rather than twisting a plane of rod-like molecules. In the same table (Table II) we report the viscosity values for MBBA¹ and those for $\text{HATXC}_{12}\text{H}_{25}$ deduced from orientational diffusivity measurements. The three $\text{HATXC}_{12}\text{H}_{25}$

TABLE I

Orientational diffusivity coefficients corresponding respectively to $\text{HATXC}_{12}\text{H}_{25}$ at 65°C, disk-like lyotropic and nematic phase (MBBA) at 25°C.

	Truxene ($\text{HATXC}_{12}\text{H}_{25}$) $T = 65^\circ\text{C}$	Disk-lyotropic phase [3]	MBBA $T \approx 25^\circ\text{C}$ [1]
$D_{\text{splay}} (\text{cm}^2 \text{s}^{-1})$	$0.59 \cdot 10^{-8}$	$1.15 \cdot 10^{-7}$	$\approx 0.56 \cdot 10^{-6}$
$D_{\text{twist}} (\text{cm}^2 \text{s}^{-1})$	$0.42 \cdot 10^{-8}$	$0.16 \cdot 10^{-7}$	$\approx 0.43 \cdot 10^{-6}$
$D_{\text{bend}} (\text{cm}^2 \text{s}^{-1})$	$1.26 \cdot 10^{-8}$	—	$\approx 4.3 \cdot 10^{-6}$
$D_{\text{splay}}/D_{\text{twist}}$	1.4	7.2	1.3
$D_{\text{bend}}/D_{\text{twist}}$	3	1?	≈ 10

TABLE II

Elastic constants and viscosity coefficients for HATXC₁₂H₂₅ at 65°C. For comparison typical values for rod-like thermotropic nematic phase are shown.

	K_{11} (dynes)	K_{22} (dynes)	K_{33} (dynes)	η_{splay} (poise)	η_{twist} (poise)	η_{bend} (poise)
Truxene						
HATXC ₁₂ H ₂₅ 65°C	$0.45 \cdot 10^{-6}$	$1.1 \cdot 10^{-6}$	$0.22 \cdot 10^{-6}$	77	270	18
MBBA ¹ 25°C	$0.35 \cdot 10^{-6}$	$\sim 0.7 \cdot 10^{-6}$	$\sim 0.7 \cdot 10^{-6}$	1.26	~ 1	0.2

viscosities are much larger than those for MBBA: $\eta_{\text{twist}}(\text{HATX})/\eta_{\text{twist}}(\text{MBBA}) \approx 270$. Furthermore η_{splay} and η_{bend} are smaller than η_{twist} : $\eta_{\text{twist}}/\eta_{\text{splay}} \sim 3$, and $\eta_{\text{twist}}/\eta_{\text{bend}} \sim 15$. This implies that the backflow effects are more important on the bend distortion than on the splay one as was habitually observed for conventional nematics.¹ The above observations may be due to the appearance of a local order of thermotropic nematic type. This order can be manifest in the packing of a few molecules (15 to 25) to form relatively short columns of a diameter of an individual disk. Each column would be equivalent to an individual rod in classical nematic LC. Consequently, similar values for the ratios $\eta_{\text{twist}}/\eta_{\text{splay}}$ and $\eta_{\text{twist}}/\eta_{\text{bend}}$ would be observed for the present system and for the rod-like thermotropic nematics. The above order (local nematic type) is confirmed by observation of X-ray diffraction from columnar disk-like phases (ordered or disordered system). The X-ray diffraction patterns show strong molecular correlations along the columns.

To conclude, we have investigated the dynamical behavior of a pure bending deformation induced by thermal fluctuations in an homeotropic nematic phase of truxene (HATX C₁₂H₂₅). Using quasi-elastic light scattering technique, with the appropriate choice of scattering geometry, with the wave vector q_z (q^{opt}) parallel to \mathbf{n}_0 , we measured the damping time associated with pure bend deformation. Furthermore, we have performed an independent measurement of K_{33} via a Frederiks transition. The experimental measurements allowed us to deduce the pure bend viscosity. So, using a previous theoretical calculation⁵ for the ratios between: K_{11} , K_{22} and K_{33} , we deduced the numerical values of K_{11} and K_{22} and those for η_{splay} and η_{twist} . The comparison of our results with those obtained in rod-like nematic phase shows that K_{11} and K_{33} interchange their role: $K_{33} > K_{11}$ for rod-like molecules and $K_{11} > K_{33}$ for discotic, K_{22} is the largest elastic constant for disk-like molecules, whereas for rod-like molecules it is the smallest one. The three curvature constants for discotic are in the same order of magnitude as those corresponding to the conventional nematic liquid crystal (N_B). This means that to produce the same distortion in nematic discotic or in nematic (N_B), one must supply the same energy. The viscosities η_{splay} , η_{twist} and η_{bend} corresponding to nematic discotic are about 2 order of magnitude larger than those corresponding to rod-like nematic (MBBA). This difference is probably due to the shape of the molecule. η_{twist} is the largest of the three viscosities. η_{splay} is weaker than η_{twist} by a ratio of the order of 3, while η_{bend} is 15 times smaller than η_{twist} .

References

1. P. G. De Gennes, *The Physics of Liquid Crystal*. Oxford (Clarendon Press) (1974).
2. S. Chandrasekhar, B. K. Sadashiva, K. A. Suresh, H. V. Madhusudana, S. Kumar, R. Shashidar and G. Ventakesh, *J. Phys. Supp. C₃*, **40**, 120 (1979). *J. Phys. Supp. C₃*, Pranama, **9**, 471 (1977).
3. M. B. Lacerda Santos, Y. Galerne and G. Durand, *J. Physique* **46**, 933–937 (1985).
4. T. Othman, M. Gharbia, A. Gharbi, C. Destrade and G. Durand, *Liq. Cryst.*, in press (1995).
5. K. Sokalski and W. Th. Ruijgrok, *Physica*, **113A**, 126 (1982).
6. P. Chatelain, *Acta Crystallographica*, **1**, 315 (1948).
7. Orsay Liquid Crystal Group, *Phys. Rev. Lett.*, **22**, 1361 (1969).
8. Groupe d'Etude des Cristaux Liquides, *J. Chem. Phys.*, **51**, 816 (1969).
9. K. Eidner, M. Lewis, H. K. M. Vithana and D. L. Johnson, *Phys. Rev. A*, **40**, 6388 (1989).
10. C. Destrade, Nguyen Huu Tinh, H. Gasparoux, J. Malthete and A. M. Levelut, *Mol. Cryst. Liq. Cryst.*, **71**, 111 (1981).
11. H. Z. Cummins and E. Rpike, Eds. *Photon Correlation and Light Beating Spectroscopy*. Plenum, New York (1977).
12. E. A. Corsellis, H. J. Coles and N. B. McKeown, Presented at the 14th International Liquid Crystal Conference, Pisa (Italy) (1992).
13. T. Warmerdam, D. Frenkel and R. J. J. Zijlstra, *J. Physique*, **48**, 319 (1987).